OPLS All-Atom Model for Amines: Resolution of the Amine Hydration Problem

Robert C. Rizzo and William L. Jorgensen*

Contribution from the Department of Chemistry, Yale University, New Haven, Connecticut 06520-8107

Received November 30, 1998. Revised Manuscript Received March 15, 1999

Abstract: Classical force-field parameters have been developed for amines primarily by fitting to experimental data for pure liquids and to hydrogen-bond strengths from gas-phase ab initio calculations. The resultant parameters were used to calculate relative free energies of hydration for ammonia, methylamine, dimethylamine, and trimethylamine using free energy perturbation calculations in Monte Carlo simulations (MC/FEP). The results including the fact that the most favorable ΔG_{hyd} occurs for methylamine are in excellent agreement with the experimental data, in contrast to numerous prior computational reports. The calculations reveal two opposing trends in water: increased contribution from hydrogen-bond acceptance and diminished contribution from hydrogen-bond donation with increasing methylation of the amines. The proper balance of hydrogen-bond strengths, which is achieved with the OPLS-AA force field, is essential for correct ordering of the free energies of hydration. MC simulations for the pure liquids of thirteen additional amines, not included in the original parametrization, then demonstrated the transferability of the force field. These simulations covered aliphatic as well as cyclic and aromatic amines. Furthermore, the appropriateness of the force field for less polar environments was confirmed through MC/FEP calculations of relative free energies of solvation and log *P* values in chloroform. It is apparent that the prior problems with classical force fields for amines were simply a result of nonoptimal parametrization rather than to a critical omission such as the lack of explicit polarization.

Introduction

Computer simulations of condensed-phase biological and organic systems in which all atoms of solutes and solvent are represented are now routine. Such computations can provide valuable characterization of molecular structure at the atomic level as well as such important thermodynamic quantities as free energies of solvation and partition coefficients.[1,2] Accurate prediction of binding affinities is also now possible and has valuable utility for rational drug design.[3−5] The most widely used methodologies are Monte Carlo (MC) and molecular dynamics (MD) simulations in conjunction with free energy perturbation (FEP) theory.[1,2,6] Generally, classical potential energy expressions (force fields) are used to evaluate the total energy,[7] and the accuracy of the results is primarily influenced by their quality. This fact underlies the philosophy of the parametrization of the OPLS (optimized potentials for liquid simulations) force fields, which recognizes the necessity of computing condensed-phase properties in the development of force fields for use in condensed-phase simulations.[8]

One particularly notable area where classical force fields have failed is in the calculation of free energies of hydration for both amines and amides.[9,10] Specifically, calculated free energies of hydration have not been in agreement with observed experimental trends for the amine series,[11,12] ammonia, methylamine, dimethylamine, and trimethylamine, and for the amide series,[13] acetamide (ACT), *N*-methylacetamide (NMA), and *N,N*-dimethylacetamide (DMA). Experimentally, these molecules show counterintuitive hydration behavior with increasing methyl substitution.[9,10] That is, one might expect that replacement of an amino hydrogen by a seemingly hydrophobic methyl group would lead to an unfavorable (positive) contribution to the free energy of hydration. In fact, the experimental data for ammonia and methylamine reveal the opposite trend with a $\Delta\Delta G_{hyd}$ of −0.26 kcal/mol.[11,12] Subsequent methylations do decrease the hydrophilic character with a $\Delta\Delta G_{hyd}$ (methylamine → dimethylamine) of +0.27 kcal/mol and a $\Delta\Delta G_{hyd}$ (dimethylamine → trimethylamine) of +1.06 kcal/mol. Furthermore, amides exhibit a similar sequence with a favorable relative free energy of hydration $\Delta\Delta G_{hyd}$ (ACT → NMA) of −0.40 kcal/mol for the first methylation, and an unfavorable $\Delta\Delta G_{hyd}$ (NMA → DMA)

(1) Kollman, P. *Chem. Rev.* **1993**, *93*, 2395−2417.

(2) Jorgensen, W. L. Free Energy Changes in Solution. In *Encyclopedia of Computational Chemistry*; Schleyer, P. v. R., Ed.; Wiley: New York, 1998; Vol. 2, p 1061−1070.

(3) Lamb, M. L.; Jorgensen, W. L. *Curr. Opin. Chem. Biol.* **1997**, *1*, 449−457.

(4) Jorgensen, W. L.; Duffy, E. M.; Essex, J. W.; Severance, D. L.; Blake, J. F.; Jones-Hertzog, D. K.; Lamb, M. L.; Tirado-Rives, J. In *Biomolecular Structure and Dynamics*; Vergoten, G., Theophanides, T., Eds.; Kluwer: Amsterdam, 1997; p 21−34.

(5) Bohm, H.-J.; Klebe, G. *Angew. Chem., Int. Ed. Engl.* **1996**, *35*, 2588−2614.

(6) Zwanzig, R. W. *J. Chem. Phys.* **1954**, *22*, 1420−1426.

(7) Allinger, N. L. Force Fields: A Brief Introduction. In *Encyclopedia of Computational Chemistry*; Schleyer, P. v. R., Ed.; Wiley: New York, 1998; Vol. 2, p 1013−1015.

(8) Jorgensen, W. L.; Maxwell, D. S.; Tirado-Rives, J. *J. Am. Chem. Soc.* **1996**, *118*, 11225−11236.

(9) Morgantini, P.-Y.; Kollman, P. A. *J. Am. Chem. Soc.* **1995**, *117*, 6057−6063.

(10) Ding, Y. B.; Bernardo, D. N.; Krogh-Jespersen, K.; Levy, R. M. *J. Phys. Chem.* **1995**, *99*, 11575−11583.

(11) Ben-Naim, A.; Marcus, Y. *J. Chem. Phys.* **1984**, *81*, 2016−2027.

(12) Jones, F. M., III; Arnett, E. M. *Prog. Phys. Org. Chem.* **1974**, *11*, 263−322.

(13) Wolfenden, R. *Biochemistry* **1978**, *17*, 201−204.

Table 1. Previously Calculated Relative Free Energies of Hydration (kcal mol^{-1}) for Amines

perturbation	FEP[a] A	FEP[b] B	polariz. FEP[c] C	FEP[d] D	polariz. FEP[d] E	SCRF GVB[e] F	exptl[f]
ammonia → methylamine	-0.07 ± 0.13	0.62 ± 0.05	0.38 ± 0.06	1.13 ± 0.19	0.3 ± 0.5	1.8	-0.26
methylamine → dimethylamine	1.93 ± 0.08	1.62 ± 0.01	1.32 ± 0.03	3.16 ± 0.25	2.5 ± 0.6	1.8	0.27
dimethylamine → trimethylamine	1.17 ± 0.06	2.34 ± 0.02	2.90 ± 0.09	2.29 ± 0.32	0.6 ± 0.6	1.5	1.06

[a] Reference 14. [b] Reference 9. [c] Reference 15. [d] Reference 10. [e] Reference 16. [f] References 11 and 12.

of $+1.53$ kcal/mol for the second methylation.[13] A general consensus does not exist concerning the physical basis of these anomalous hydration trends.

Previous Simulation Studies. Given the biological importance of the amide and amine functional groups, numerous computer simulations have been performed in an effort to study the anomalous hydration patterns. For focusing on the amines, computational studies have employed standard classical potential-energy functions and polarizable potential functions in MD simulations with explicit solvent molecules, and self-consistent reaction field (SCRF) methods.[9,10,14−17] However, all of the MD and most of the SCRF calculations have yielded serious discrepancies with the experimental data (Table 1). Early studies by Rao and Singh[14] used MD/FEP calculations with an all-atom AMBER force field to obtain the results for the amine series in Table 1, column A. Although the computed relative free energies obtained for the first and third methylations are close to the experimental values, the second methylation yielded a $\Delta\Delta G$ of 1.93 kcal/mol, much higher than the experimental result of 0.27 kcal/mol. This study also suffered from large hystereses in the computed van der Waals (Lennard-Jones) component of the free energy change and short simulation times. Kollman and co-workers also used MD/FEP methods and found significant disagreement between calculated and experimental values for the amines using both the pairwise-additive AMBER 4.0 potentials[9] and a fully polarizable model[15] (Table 1, columns B and C). The simulations consistently revealed increasingly positive $\Delta\Delta G$s with increasing methyl substitution. Likewise, Ding et al.[10] used MD/FEP methods to calculate $\Delta\Delta G_{hyd}$ for the amine series with and without polarization (Table 1, columns D and E). The errors are again large; although polarization seems to provide some improvement, the error for the methylamine to dimethylamine transformation is still greater than 2 kcal/mol.

Subsequently, Marten et al.[16] tried SCRF calculations with a polarizable quantum-mechanical solute and a dielectric continuum representation of the solvent. Despite the more sophisticated treatment of the solute, the computed relative free energies of hydration obtained were essentially constant at 1.5−1.8 kcal/mol, once again in significant disagreement with the experimental data (Table 1, column F). These researchers were able to reproduce the observed hydration results only by including a hydrogen-bond correction term to fit the experimental data.[16] Barone et al. have recently noted the sensitivity of SCRF results to the choice of atomic radii.[17b] Notably, Marten at al.[16] also reported hydrogen-bond strengths for the amines with a water molecule as both donor and acceptor using two force fields (OPLS* and AMBER*) and ab initio LMP2/cc-pVTZ(-f) calculations. The authors concluded that hydrogen-

bonding interactions are improperly modeled by the force fields. In particular, the amines are too good as hydrogen-bond donors and the nearly constant acceptor strength is not reproduced with the force fields. It should be noted that OPLS parameters have only been reported previously for primary amines.[8,18] The OPLS* parameters used in the MacroModel program and other "OPLS" parameters[10] for secondary and tertiary amines were not developed in our laboratory.

Because of the success in reproducing experimental free energies of hydration using FEP methods for numerous organic molecules,[19] the discrepancy between theory and experiment for the amines is troublesome. In addition, the widespread interest in structure-based drug design necessitates accurate models for amines since they are very common components in drugs. In this paper, OPLS-AA (all-atom) parameters are reported for ammonia and for primary, secondary, and tertiary amines. As usual, the development has considered molecular structures, conformational energetics, hydrogen bonding, pure liquid properties, and relative free energies of hydration. The number of new parameters is kept to a minimum. The parameter set was developed for ammonia, methylamine, dimethylamine, and trimethylamine. Subsequent testing covered a variety of additional primary, secondary, and tertiary amines including cyclic and aromatic amines. Simulations in chloroform were also carried out for the four key amines in order to test the suitability of the parameters in less polar environments. This permitted computation of relative free energies of transfer and comparison with experimental partition coefficients, log P.

Computational Methods

Force Field and Parametrization. The potential energy function consists of harmonic bond-stretching and angle-bending terms, a Fourier series for torsional energetics, and Coulomb and Lennard-Jones terms for the nonbonded interactions, eqs 1−4.[8]

$$E_{bond} = \sum_i k_{b,i}(r_i - r_{0,i})^2 \tag{1}$$

$$E_{angle} = \sum_i k_{\vartheta,i}(\vartheta_i - \vartheta_{0,i})^2 \tag{2}$$

$$E_{torsion} = \sum_i \left[\frac{1}{2}V_{1,i}(1 + \cos\varphi_i) + \frac{1}{2}V_{2,i}(1 - \cos 2\varphi_i) + \frac{1}{2}V_{3,i}(1 + \cos 3\varphi_i) \right] \tag{3}$$

$$E_{non-bond} = \sum_i \sum_{j>i} \left\{ \frac{q_i q_j e^2}{r_{ij}} + 4\epsilon_{ij}\left[\left(\frac{\sigma_{ij}}{r_{ij}}\right)^{12} - \left(\frac{\sigma_{ij}}{r_{ij}}\right)^6 \right] \right\} \tag{4}$$

The parameters are the force constants k, the r_0 and ϑ reference values, the Fourier coefficients V, the partial atomic charges q and the Lennard-Jones radii and well-depths, σ and ϵ. Standard combining rules are used such that $\sigma_{ij} = (\sigma_{ii}\sigma_{jj})^{1/2}$ and $\epsilon_{ij} = (\epsilon_{ii}\epsilon_{jj})^{1/2}$.[8] The nonbonded

(14) Rao, B. G.; Singh, U. C. *J. Am. Chem. Soc.* **1989**, *111*, 3125−3133.

(15) Meng, E. C.; Caldwell, J. W.; Kollman, P. A. *J. Phys. Chem.* **1996**, *100*, 2367−2371.

(16) Marten, B.; Kim, K.; Cortis, C.; Friesner, R. A.; Murphy, R. B.; Ringnalda, M. N.; Sitkoff, D.; Honig, B. *J. Phys. Chem.* **1996**, *100*, 11775−11788.

(17) (a) Cramer, C. J.; Truhlar, D. G. *J. Comput.-Aided Mol. Des.* **1992**, *6*, 629−666. (b) Barone, V.; Cossi, M.; Tomasi, J. *J. Chem. Phys.* **1997**, *107*, 3210−3221. (c) Klamt, A.; Jonas, V.; Bürger, T.; Lohrenz, J. C. W. *J. Phys. Chem. A* **1998**, *102*, 5074−5085.

(18) Jorgensen, W. L.; Briggs, J. M.; Contreras, M. L. *J. Phys. Chem.* **1990**, *94*, 1683−1686.

(19) (a) Sun, Y.; Spellmeyer, D.; Pearlman, D. A.; Kollman, P. *J. Am. Chem. Soc.* **1992**, *114*, 6798−6801. (b) Jorgensen, W. L.; Tirado-Rives, J. *Perspect. Drug Discovery Des.* **1995**, *3*, 123−138.

Resolution of the Amine Hydration Problem

J. Am. Chem. Soc., Vol. 121, No. 20, 1999 4829

interactions are evaluated intermolecularly and for intramolecular atom pairs separated by three or more bonds. The 1,4-intramolecular interactions are reduced by a factor of 2 in order to use the same parameters for both intra- and intermolecular interactions.[8]

Standard bond-stretching and angle-bending parameters were initially assigned from the OPLS-AA parameter set,[8] which includes many entries from the AMBER all-atom force field.[20] Each atom has an associated AMBER atom type that is used to designate the parameters for atom pairs (bond stretching) or atom triplets (angle bending). The AMBER atom types used here are NT (amine nitrogen), H (hydrogen on nitrogen), CT (aliphatic carbon), HC (hydrogen on aliphatic carbon), CA (aromatic carbon), and HA (hydrogen on aromatic carbon). The present work then focused on the development of the Fourier coefficients, partial charges, and Lennard-Jones parameters.

Parametrization is an iterative process. First, a Z-matrix was constructed for each amine, and initial parameters were assigned on the basis of the published values for primary amines.[8] Replacement of amino hydrogens by OPLS-AA methyl groups yielded trial partial charges for secondary and tertiary amines, and initial parameters for ammonia were taken from the work of Gao et al.[21] Gas-phase energy minimizations were then performed with the BOSS program[22] with the use of these parameters. The geometries obtained were compared with those from experiments and from ab initio optimizations at the RHF/6-31G* level. This provided a basis for adjusting the parameters for bond stretching and angle bending. The ab initio calculations were performed with Gaussian 95.[23] The procedure for determination of missing Fourier coefficients has been described.[8] Briefly, an energy scan was performed for examples of the missing torsions with RHF/6-31G* calculations. A full geometry optimization was done at each point with the exception of the chosen dihedral angle. Similarly, the same energy scans were carried out using the force field with the BOSS program and with the Fourier coefficients for the missing torsion set to zero. Then, the relative energies from the scans are used as input to the Simplex-based fitting program, Fitpar,[24] to determine the Fourier coefficients that minimize the differences between the RHF/6-31G* and force-field results. The initial Fourier coefficients often require refitting when the atomic charges and Lennard-Jones parameters are subsequently adjusted.

The observation of Marten et al.[16] concerning the flawed representation of hydrogen bonding of amines with water guided our early assignments of the partial charges for amines. The charges for H(N), N, and C were adjusted to reproduce the LMP2 interactions energies for each complex of the four prototypical amines with a water molecule.[16] For comparison, we also computed the corresponding interaction energies at the RHF/6-31G* level. In each case, all degrees of freedom were optimized. However, it was necessary to constrain the hydrogen bonds to be linear for the RHF/6-31G* calculations in which water was the hydrogen-bond acceptor, to avoid rearrangements.

When satisfactory agreement with molecular structures, torsional energy scans, and hydrogen-bond strengths was obtained, MC simulations for the four pure liquids were performed. Some adjustments of the partial charges and Lennard-Jones parameters were made so that calculated properties for the pure liquid amines agreed well with experiment. In general, the computed heats of vaporization are most

affected by the choice of partial charges, while densities are particularly sensitive to the Lennard-Jones radii. Since our efforts were guided by consideration of multiple types of experimental and ab initio data, the final parameter set reflects a compromise. If satisfactory results had not been obtained with the OPLS-AA model, we would have considered augmentation with an extra interaction site in a lone-pair position on nitrogen. This turned out not to be necessary. We did not expect that explicit polarization would be needed in view of the prior successes with so many other organic liquids and water.[8,25]

Pure Liquid Simulations. The Metropolis Monte Carlo simulations[26] were performed with the BOSS program on Silicon Graphics workstations or a multiprocessor Pentium cluster running Linux. All molecules were fully flexible, which necessitates that MC simulations be performed for both the ideal gas and liquid in order to compute heats of vaporization, ΔH_{vap}. The calculations were executed in the NPT ensemble at 1 atm and at either the normal boiling point of the liquid or at 25 °C. Gas-phase simulations consisted of 3×10^6 configurations of equilibration, followed by 3×10^6 configurations of averaging. For the pure liquids, periodic boundary conditions were employed with cubic cells of 267 molecules. The equilibrated box sizes ranged from approximately $22 \times 22 \times 22$ Å for ammonia to $40 \times 40 \times 40$ Å for triethylamine. Intermolecular nonbonded interactions were truncated at 11 Å, based roughly on the center-of-mass of each molecule, and quadratically feathered to zero over the last 0.5 Å. For nonaqueous solvents, a standard correction is made for Lennard-Jones interactions neglected beyond the cutoff.[27] Each liquid was first equilibrated for 12×10^6 configurations and the averaging occurred over an additional 12×10^6 configurations, which were run in batches of 5×10^5 configurations. Statistical uncertainties ($\pm 1\sigma$) were obtained through the batch means procedure (eq 5)

$$\sigma^2 = \sum_i^m (\theta_i - \langle\theta\rangle)^2/m(m-1) \qquad (5)$$

where m is the number of batches and θ_i is the average of property θ in the ith batch.[27] Overall, the computed densities, heats of vaporization, radial distribution functions, energy distributions and conformational properties are very well converged with MC simulations of this length. By adjusting the allowed ranges for rigid-body rotations, translations, and dihedral angle movement, acceptance ratios of between 40% for aliphatic amines and 18−20% for cyclic and aromatic amines were obtained for new configurations. The ranges for bond stretching and angle bending are set automatically by the BOSS program on the basis of the force constants and temperature.

It should be noted that more than one set of nonbonded parameters may yield calculated densities and heats of vaporization in close agreement with experiment. For ammonia, 25 pure liquid simulations were run using different nonbonded parameter sets. Six of these yielded a calculated density and heat of vaporization within 3% of the experimental values. Only parameter sets for ammonia were further considered if they also yielded reasonable hydrogen-bond energetics with water and a qualitatively correct free energy of hydration relative to methylamine. Otherwise, free energies of hydration were not considered in the parametrization.

Free Energy Perturbations. As an example, the relative free energies of hydration for methylamine and ammonia can be determined from the thermodynamic cycle in Figure 1, which leads to eq 6.[18,28]

$$\Delta\Delta G_{hyd} = \Delta G_{water} - \Delta G_{gas} = \Delta G_{hyd}(NH_3) - \Delta G_{hyd}(CH_3NH_2) \qquad (6)$$

ΔG_{gas} is evaluated here through MC/FEP simulations by mutation of

(20) Cornell, W. D.; Cieplak, P.; Bayly, C. I.; Gould, I. R.; Merz, K. M.; Ferguson, D. M.; Spellmeyer, D. C.; Fox, T.; Caldwell, J. W.; Kollman, P. A. *J. Am. Chem. Soc.* **1995**, *117*, 5179−5197.
(21) Gao, J. L.; Xia, X.; George, T. F. *J. Phys. Chem.* **1993**, *97*, 9241−9247.
(22) Jorgensen, W. L. *BOSS Version 3.8*; Yale University: New Haven, CT, 1997.
(23) Frisch, M. J.; Trucks, G. W.; Schlegel, H. B.; Scuseria, G. E.; Robb, M. A.; Cheeseman, J. R.; Strain, M. C.; Burant, J. C.; Stratman, R. E.; Petersson, G. A.; Montgomery, J. A.; Zakrzewski, V. G.; Raghavachari, K.; Ayala, P. Y.; Cui, Q.; Morokuma, K.; Ortiz, J. V.; Foresman, J. B.; Cioslowski, J.; Stefanov, B. B.; Chen, W.; Wong, M. W.; Andres, J. L.; Replogle, E. S.; Gomperts, R.; Martin, R. L.; Fox, D. J.; Keith, T.; Al-Laham, M. A.; Nanayakkara, A.; Challacombe, M.; Peng, C. Y.; Stewart, J. J. P.; Gonzalez, C.; Head-Gordon, M.; Gill, P. M. W.; Johnson, B. G.; Pople, J. A. *Gaussian 95, Development Version (Revision E.1)*; Gaussian Inc.: Pittsburgh, PA, 1996.
(24) Maxwell, D.; Tirado-Rives, J. *Fitpar Version 1.1.1.*; Yale University: New Haven, Connecticut, 1994.
(25) Jorgensen, W. L.; Chandrasekhar, J.; Madura, J. D.; Impey, R. W.; Klein, M. L. *J. Chem. Phys.* **1983**, *79*, 926−935.
(26) Metropolis, N.; Rosenbluth, A. W.; Rosenbluth, M., N.; Teller, A. H. *J. Chem. Phys.* **1953**, *21*, 1087−1092.
(27) Jorgensen, W. L. Monte Carlo Simulations of Liquids. In *Encyclopedia of Computational Chemistry*; Schleyer, P. v. R., Ed.; Wiley: New York, 1998; Vol. 3, p 1754−1763.
(28) Jorgensen, W. L.; Ravimohan, C. *J. Chem. Phys.* **1985**, *83*, 3050−3054.
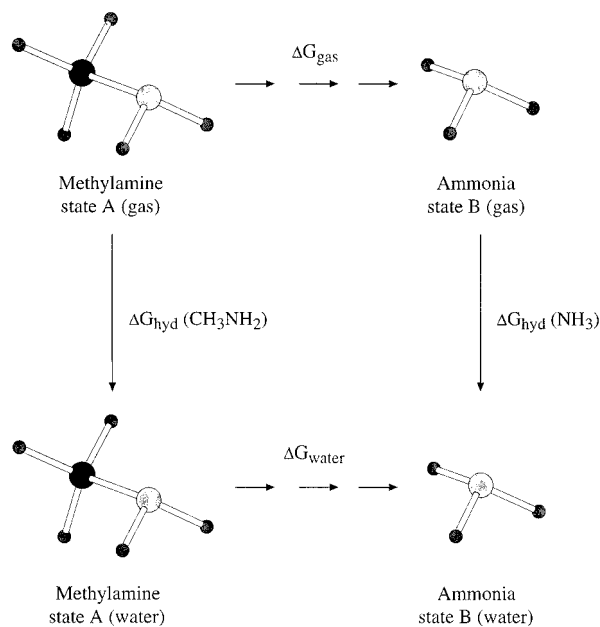
Figure 1. The thermodynamic cycle used to determine the relative free energy of hydration ($\Delta\Delta G_{hyd}$) of methylamine and ammonia.

methylamine to ammonia in isolation, and ΔG_{water} is obtained by an equivalent mutation in the presence of explicit water molecules. Their difference can then be compared to the difference in experimental free energies of hydration. The free energy change for conversion of molecule A to B is computed via eq 7,

$$\Delta G(A \rightarrow B) = G_B - G_A = -k_bT \ln\langle\exp[-(E_B - E_A)/k_bT]\rangle_A \quad (7)$$

where k_b is Boltzmann's constant, T is the temperature, E is the total potential energy for the full system with A or B, and the averaging is performed for system A.[6] To promote convergence, a coupling parameter λ is introduced to allow gradual interconversion of the potential functions and geometries, ξ, of A and B (eq 8).

$$\xi(\lambda) = \lambda\zeta_B + (1 - \lambda)\xi_A \quad (8)$$

Several incremental mutations are performed between $\lambda = 0$ (A) and $\lambda = 1$ (B). A typical $\Delta\lambda$ is ±0.05, which requires 10 separate simulations (windows) for the full mutation using double-wide sampling.[28] Frequently however, smaller $\Delta\lambda$ values are used near the end points of the mutations, where the free energy changes are often largest or noisiest. All of the present free energy perturbations consisted of mutating a methyl group to a hydrogen atom. The three methyl hydrogens are mutated to dummy atoms, which have zero for q, σ, and ϵ, and the methyl carbon is mutated to the appropriate secondary, primary, or ammonia hydrogen, H(NT). For these fully flexible systems, we retain the CT−HC force constants for the H(NT)-dummy pairs, but reduce the r_0 to 0.3 Å. For the angle bending, we retain only one angle to the dummy atom with nonzero parameters. This combination keeps the dummy atom in a reasonable position without placing any constraint on the final structure, that is, the same total energy is obtained from an energy minimization with or without the dummy atoms.[29]

The use of flexible geometries for the solutes requires computation of ΔG_{gas} in Figure 1. In this case, the MC simulation for each window consisted of 3×10^6 configurations of equilibration followed by 3×10^6 configurations of averaging. The ranges for dihedral-angle changes were adjusted so that ca. 40% acceptance for new configurations was achieved. Convergence was monitored by plotting the results for ΔG_{gas} vs λ, which showed little change after 1×10^6 configurations of averaging.

The FEP calculations in water were performed for a single solute in a periodic cube with 500 TIP4P water molecules.[25] Both solute−solvent

(29) Severance, D. L.; Essex, J. W.; Jorgensen, W. L. *J. Comput. Chem.* **1995**, *16*, 311−327.

Table 2. OPLS-AA Bond Stretching Parameters

bond	k_b (kcal mol^{-1} Å^{-2})	r_0 (Å)
H−NT	434.0	1.010
CA−NT	481.0	1.340
CT−NT	382.0	1.448
CA−HA	367.0	1.080
CT−HC	340.0	1.090
CT−CT	268.0	1.529
CA−CA	469.0	1.400

Table 3. OPLS-AA Angle-Bending Parameters

angle	k_θ (kcal mol^{-1} rad^{-2})	θ_0 (deg)
CT−NT−H	35.00	109.50
H−NT−H	43.60	106.40
CA−NT−H	35.00	111.00
CA−CA−NT	70.00	120.10
CA−NT−CT	50.00	109.50
CA−CA−HA	35.00	120.00
CA−CA−CA	63.00	120.00
CT−CT−HC	37.50	110.70
CT−CT−CT	58.35	112.70
HC−CT−HC	33.00	107.80
CT−CT−NT	56.20	109.47
CT−NT−CT	51.80	107.20
HC−CT−NT	35.00	109.50

and solvent−solvent cutoffs were at 10.0 Å based roughly on the separations of amine nitrogens and water oxygens. Each window consisted of 6×10^6 configurations of equilibration, followed by 8×10^6 configurations of averaging. Negligible differences in the computed free energy changes occurred after 5×10^6 configurations of averaging. Similarly, as in the pure liquid simulations, adjustment of the allowed ranges for rigid body rotations, translations, and dihedral angle movements yielded acceptance rates of 30−50% for new configurations. The simulation protocol in chloroform was the same except that the number of chloroform molecules was 267 and the solvent−solvent and solute−solvent cutoffs were extended to 12.0 Å. The potential functions for chloroform are the OPLS 4-site model.[18]

Results and Discussion

Parameters. The final OPLS-AA parameters for amines are reported in Tables 2−5. The bond-stretching and angle-bending parameters (Tables 2 and 3) are mostly from prior work.[8] Missing combinations of atom types for aromatic amines, for example, the CA−NT bond-stretching and CA−NT−H, CA−CA−N, and CA−NT−CT angle-bending parameters, were extrapolated from related types and adjusted to yield good accord with RHF/6-31G* optimized geometries. As before,[8] the molecular structures from OPLS-AA optimizations are essentially identical to RHF/6-31G* results; for bond lengths and bond angles involving nitrogen, the average deviations are 0.01 and 1.5°. Furthermore, the average differences between the computed results and experimental data are 0.02 Å for bond lengths and 2° for bond angles.

The torsional parameters are listed in Table 4. The parameters for primary amines and hydrocarbons were reported previously and are provided for completeness.[8] Additional torsional parameters were developed in this work for the HC−CT−NT−CT and CT−NT−CT−CT combinations in aliphatic amines and for the CA−CA−NT−H and CA−CA−NT−CT torsions in anilines. The OPLS-AA parameters reproduce all tested RHF/6-31G* torsional-energy profiles with an average difference of less than 0.1 kcal/mol for methylamine (HCNH), ethylamine (CCNH, HCCN), propylamine (CCNH, CCCN), dimethylamine (HCNC), diethylamine (CCNC), trimethylamine (HCNC), and triethylamine (CCNC).

Table 4. OPLS-AA Fourier Coefficients (kcal mol^{-1})

amine type	dihedral angle	V_1	V_2	V_3
aliphatic	HC−CT−NT−H	0.000	0.000	0.400
aliphatic	HC−CT−CT−NT	−1.013	−0.709	0.473
aliphatic	CT−CT−NT−H	−0.190	−0.417	0.418
aliphatic	CT−CT−CT−NT	2.392	−0.674	0.550
aliphatic	CT−NT−CT−CT	0.416	−0.128	0.695
aliphatic	HC−CT−NT−CT	0.000	0.000	0.560
aliphatic	HC−CT−CT−HC	0.000	0.000	0.318
aliphatic	HC−CT−CT−CT	0.000	0.000	0.366
aliphatic	CT−CT−CT−CT	1.740	−0.157	0.279
four-member cyclic	CT−CT−NT−H	0.000	4.000	0.000
five-member cyclic	CT−CT−NT−H	0.200	−0.417	0.418
six-member cyclic	CT−CT−NT−H	0.819	−0.417	0.418
exocyclic methyl group	CT−NT−CT−CT	1.536	−0.128	0.695
aromatic	CA−CA−NT−H	0.000	2.030	0.000
aromatic	CA−CA−NT−CT	−7.582	3.431	3.198
aromatic (improper)	Z−CA−X−Y	0.000	2.200	0.000
aromatic	X−CA−CA−Y	0.000	7.250	0.000

Table 5. OPLS-AA Non-Bonded Parameters

atom type	atom or group	q (e$^-$)	σ (Å)	ϵ (kcal mol^{-1})
NT	ammonia	−1.02	3.42	0.170
NT	1° amine	−0.90	3.30	0.170
NT	2° amine	−0.78	3.30	0.170
NT	3° amine	−0.63	3.30	0.170
H(NT)	ammonia	0.34	0.00	0.000
H(NT)	1° amine	0.36	0.00	0.000
H(NT)	2° amine	0.38	0.00	0.000
HC(CT)	for CT directly bonded to NT	0.06	2.50	0.015
HC	alkanes	0.06	2.50	0.030
CT(NT)	1° amine CH$_3$ group	0.00	3.50	0.066
CT(NT)	2° amine CH$_3$ group	0.02	3.50	0.066
CT(NT)	3° amine CH$_3$ group	0.03	3.50	0.066
CT(NT)	1° amine CH$_2$ group	0.06	3.50	0.066
CT(NT)	2° amine CH$_2$ group	0.08	3.50	0.066
CT(NT)	3° amine CH$_2$ group	0.09	3.50	0.066
CA(NT)	1° amine ipso carbon	0.18	3.55	0.070
CA(NT)	2° amine ipso carbon	0.20	3.55	0.070
CA(NT)	3° amine ipso carbon	0.21	3.55	0.070

It was found that cyclic aliphatic amines required unique CT−CT−NT−H and CT−NT−CT−CT torsional terms in order to obtain close agreement with ab initio results for equatorial vs axial disposition of hydrogens or methyl groups on nitrogen in cyclic amines. With the reported parameters, there is reasonable

equatorial   axial
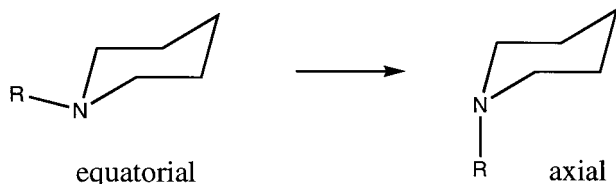
accord among the computed results; for example, for piperidine and *N*-methylpyrrolidine the equatorial conformers are preferred by 0.82 and 2.61 kcal/mol with the force field, 0.82 and 3.68 kcal/mol with RHF/6-31G*//RHF/6-31G*, and 0.36 and 3.44 kcal/mol with B3LYP/6-31G*//RHF/6-31G*. For piperidine, higher-level ab initio calulations give values of 0.6−0.9 kcal/mol, and experimental results are 0.2−0.5 kcal/mol.[30]

The torsional parameters, which were developed for a monosubstituted functional group, are then also used for polysubstituted cases. Although this is generally successful, *N,N*-dimethylaniline initially semed problematic. Although nearly exact agreement was obtained between the OPLS-AA and RHF/6-31G* dihedral-angle energy profiles for both aniline and *N*-methylaniline, the RHF/6-31G* torsion scan for the tertiary analogue yields a rotational barrier of 0.6 kcal/mol, while the force field gives a barrier of 2.2 kcal/mol. These values are lower than the barriers of ca. 3.7 kcal/mol for aniline and *N*-methylaniline from both OPLS-AA and RHF/6-31G*. Estimates from experimental sources have not converged, but are in the 3−6 kcal/mol range for all three anilines.[31] To investigate the possibility that electron correlation may be important, the dimethylaniline scan was repeated with B3LYP/6-31G* optimizations. This did yield a higher barrier, 3.5 kcal/mol, and the reported CA−CA−NT−CT parameters have been retained for both secondary and tertiary anilines.

The nonbonded parameters for amines are listed in Table 5. The pattern of partial charges was largely determined by reproduction of the hydrogen-bond strengths (vide infra). The

partial negative charge on nitrogen becomes more positive by 0.12−0.15 *e* for each added methyl group, and the charge on the amine hydrogen becomes more positive by 0.02 *e* on going from ammonia to primary and then secondary amines. The charge for hydrogens on α-carbons was fixed at 0.06 *e* and this then determined from neutrality the required charges on the α-carbons. The same charges are used for anilines with neutrality determining the charge for ipso carbons. Thus, only the charges on N and H(N) were effectively varied and the results form simple patterns. The charge on nitrogen in ammonia, −1.020 *e*, ended up only slightly different from Gao's value of −1.026 *e*,[20] which may reflect the change to a flexible geometry.

The Lennard-Jones parameters in Table 5 remained unchanged from the original OPLS-AA parameter set[8] with minor exceptions. For ammonia, the Lennard-Jones σ needed adjustment to obtain satisfactory agreement with both the experimental density and heat of vaporization of the pure liquid. Otherwise, the Lennard-Jones parameters for nitrogens in all amines are the same with σ = 3.30 Å and ϵ = 0.17 kcal/mol, whereas 3.25 Å and 0.17 kcal/mol had previously been used for primary amines.[8] The σ and ϵ for amine hydrogens are zero, as always for hydrogens attached to heteroatoms.[8] And, for hydrogens on α-carbons, the reduced ϵ of 0.015 kcal/mol has been used vs 0.030 for alkanes. The same reduced ϵ is used for α hydrogens in aldehydes, ketones, esters, and nitro compounds.[8] All parameters for more remote alkyl and aromatic carbons and hydrogens have the standard OPLS-AA values.[8] Thus, it turns out that there is little new in Table 5 beyond the choice of charges for N and H(N) in amines.

Gas-Phase Interaction Energies. The hydrogen-bond strengths for the amine−water complexes from the OPLS*, AMBER*, and ab initio LMP2 calculations of Marten et al.[16] are listed in Table 6 along with the present RHF/6-31G* and OPLS-AA results. It is expected that the LMP2 results are highly accurate,[32] so that they provide the target patterns for the force fields. Qualitatively, the LMP2 and RHF/6-31G* results show the same trends, a nearly constant interaction energy around −6 kcal/mol for water as the hydrogen-bond donor and a significantly weaker interaction of −2 to −3 kcal/mol for water as the hydrogen-bond acceptor. The incorrect orderings from the MacroModel calculations are well-remedied by the OPLS-AA results. The hydrogen bonds are uniformly 20−30% stronger

(30) (a) St. Amant, A.; Cornell, W. D.; Kollman, P. A.; Halgren, T. A. *J. Comput. Chem.* **1995**, *16*, 1483−1506. (b) Lambert, J. B.; Featherman, S. I. *Chem. Rev.* **1975**, *75*, 611−626. (c) Blackburne, I. D.; Katritzky, A. R.; Takeuchi, Y. *Acc. Chem. Res.* **1975**, *8*, 300−306.

(31) Anet, F. A. L.; Ghiaci, M. *J. Am. Chem. Soc.* **1979**, *101*, 6857−6860.

(32) Murphy, R. B.; Beachy, M. D.; Friesner, R. A.; Rignalda, M. N. *J. Chem. Phys.* **1995**, *103*, 1481−1490. Kim, K.; Friesner, R. A. *J. Am. Chem. Soc.* **1997**, *119*, 12952−12961.

Table 6. Comparison of Hydrogen-Bond Interaction Energies (kcal mol^{-1}) for Amines

molecule	previously reported[a]			this study	
	OPLS*[b]	AMBER*[b]	LMP2	RHF[c]	OPLS-AA
		Water as a H-Bond Donor			
ammonia	−7.5	−9.7	−5.5	−6.6	−6.5
methylamine	−7.0	−7.6	−5.9	−6.5	−7.4
dimethylamine	−6.3	−5.4	−6.1	−6.3	−7.8
trimethylamine	−5.1	−3.0	−6.1	−5.9	−7.5
		Water as a H-Bond Acceptor			
ammonia	−4.2	−6.1	−2.2	−2.9	−3.1
methylamine	−4.4	−7.3	−2.3	−2.7	−3.6
dimethylamine	−4.6	−8.4	−2.4	−2.7	−3.8

[a] Reference 16. [b] Asterisk denotes MacroModel version. [c] RHF/6-31G*//RHF/6-31G* optimizations with water fixed: r(OH) = 0.9572 Å and ∠HOH = 104.52°. For water as hydrogen-bond donor, six intermolecular degrees of freedom were optimized. For water as hydrogen-bond acceptor, the H-bond was constrained to be linear.
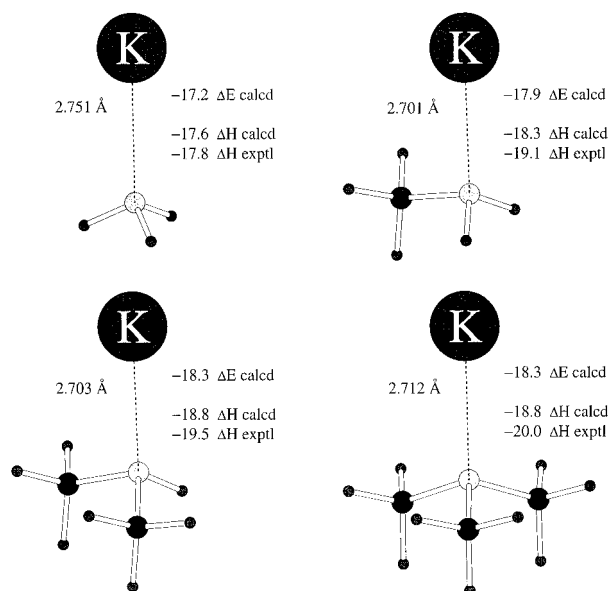
Figure 2. Gas-phase interaction energies and enthalpies (kcal/mol) of amines with potassium ion. Calculated results are from the OPLS-AA force field, and the experimental enthalpies are from ref 58.

with the OPLS-AA force field than from the LMP2 calculations. Such enhancement of intermolecular interactions is needed for reproduction of, for example, heats of vaporization with the fixed charge models.[8,25] This presumably compensates for the lack of explicit polarization. As an additional check of the robustness of the force field, enthalpies of interaction were computed from normal mode calculations for ammonia, methylamine, dimethylamine, and trimethylamine with potassium ion using Åqvist's K$^+$ parameters.[33] Excellent agreement with gas-phase experimental data was obtained, as shown in Figure 2.

Pure Liquid Results. The OPLS-AA parameters for ammonia, methylamine, dimethylamine, and trimethylamine were developed in conjunction with computation of their liquid densities and heats of vaporization. These are considered to be the key properties since they reflect both the size of the molecules and the average intermolecular interactions. The transferability of the parameters was tested through subsequent MC simulations for the pure liquids of ethylamine, propylamine, diethylamine, triethylamine, aziridine, azetidine, pyrrolidine, 1-methylpyrrolidine, piperidine, 1-methylpiperidine, aniline, *N*-methylaniline, and *N,N*-dimethylaniline. The results are shown

(33) Åqvist, J. *J. Phys. Chem.* **1990**, *94*, 8021−8024.

in Table 7. In all cases, excellent agreement with experimental densities was obtained with an average unsigned error of 1%.

Heats of vaporization are readily computed from the simulation results using eq 9.

$$\Delta H_{\text{vap}} = H_{\text{gas}} - H_{\text{liquid}} = E_{\text{intra}}(\text{gas}) - E_{\text{tot}}(\text{liquid}) + RT \quad (9)$$

Here, E_{intra}(gas) is the average intramolecular energy in the gas-phase, and E_{tot} (liquid) is the total potential energy of the liquid consisting of both the average intramolecular energy of the liquid, E_{intra}(liquid), and the average intermolecular energy of the liquid, E_{inter}(liquid). The *PV*-work term in the enthalpy is equal to RT for the ideal gas and it is negligible for the liquid. The heats of vaporization obtained from the MC simulations for the gases and liquids are also in good agreement with the experimental data in Table 7; the average unsigned error is less than 3%.

Piperidine is an interesting case. The pure liquid simulations were normally started using the lowest-energy conformation for all molecules as determined from the gas-phase energy minimizations with the new force field. While acyclic aliphatic and aromatic amines pose no sampling problems with respect to the intramolecular degrees of freedom, cyclic aliphatic compounds tend to stay in the original ring conformation, since ring flipping or inversion barriers are ca. 6 kcal/mol. Although, as mentioned above, the force field favors equatorial piperidine by 0.8 kcal/mol over the axial form in the gas phase, pure liquid simulations were run, starting from both conformers, for all piperidine molecules in the liquid. At the ends of the runs, no molecules had changed conformation in the equatorial liquid, while only three of the initially axial molecules were equatorial. The results in Table 7 show that the calculated densities for the axial and equatorial liquids are nearly the same and both are very close to the experimental value of 0.857 g cm^{-3}. However, the calculated heat of vaporization is higher than the experimental value by 1.3 kcal/mol for the equatorial liquid, while it is too low by 0.7 kcal/mol for the axial liquid. In both cases the gas is taken as equatorial. The comparison between theory and experiment suggests that piperidine in the pure liquid is a mixture of equatorial and axial. The exact mixture could be pursued with a modified MC sampling procedure that can achieve the equilibrium, although the acceptance rate may be low. On the experimental side, the conformational preference for piperidine has been the subject of lively debate.[31] The conclusion from numerous spectroscopic measurements is that piperidine is equatorial in the gas phase and in nonpolar solvents but that it is mostly axial in alcohol solvents. The possibility of a mixture for the neat liquid near 25 °C seems reasonable. It may also be noted that for 1-methylpiperidine, the computed and experimental results in Table 7 show the usual level of accord. In this case, the evidence is that the equatorial form is dominant in all media.[31]
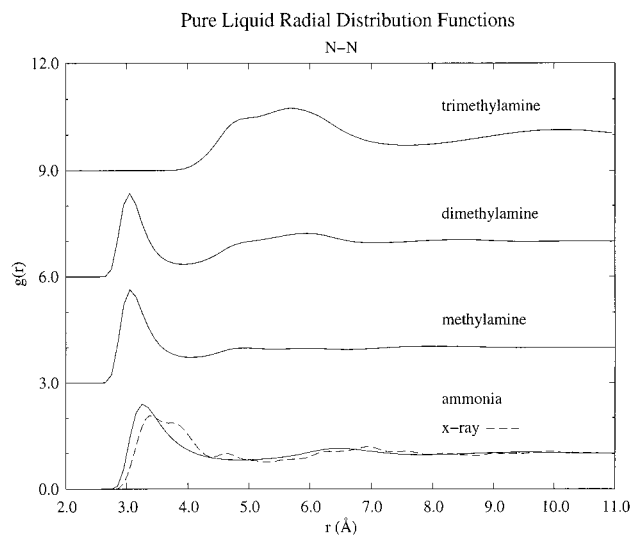
Radial distribution functions (rdfs) provide a measure of the local structure in liquids and coordination numbers can be obtained by the integration of their peaks.[27] The N−N rdfs for the four prototypical amines are presented in Figure 3. The loss of hydrogen bonding for trimethylamine is clearly apparent in the lack of a peak near 3 Å. Estimates of the numbers of hydrogen bonds per molecule are more readily obtained from integration of the first peak in the N−H(N) rdfs, which reveal sharper first peaks with minima near 2.5 Å (not shown). Integration to that point yields average numbers of hydrogen bonds of 2.56 for ammonia at −33 °C, 1.96 for methylamine at −6 °C, and 1.11 for dimethylamine at 7 °C. The latter figure is consistent with the expected hydrogen-bonded chains, while

Table 7. Computed Densities and Heats of Vaporization from Pure Liquid Simulations

liquid	T (°C)	density (g cm^{-3})		ΔH_{vap} (kcal mol^{-1})	
		calcd	exptl	calcd	exptl
ammonia	−33.35	0.697 ± 0.001	0.682[a]	5.42 ± 0.008	5.58[a]
methylamine	−6.30	0.698 ± 0.002	0.694[b]	6.22 ± 0.018	6.17[c]
ethylamine	16.50	0.705 ± 0.002	0.687[d]	6.95 ± 0.023	6.70[e]
propylamine	25.00	0.717 ± 0.001	0.711[f]	7.80 ± 0.030	7.47[g]
dimethylamine	6.88	0.658 ± 0.002	0.671[d]	6.22 ± 0.024	6.33[h]
diethylamine	25.00	0.709 ± 0.001	0.699[i]	7.84 ± 0.021	7.48[g]
trimethylamine	2.87	0.660 ± 0.001	0.653[d]	5.32 ± 0.021	5.48[j]
triethylamine	25.00	0.722 ± 0.001	0.723[d]	8.61 ± 0.028	8.33[g]
aziridine	25.00	0.802 ± 0.001	0.831[k]	8.20 ± 0.020	8.09[l]
azetidine	25.00	0.820 ± 0.001	0.841[m]	7.77 ± 0.020	8.17[l]
pyrrolidine	25.00	0.860 ± 0.001	0.854[n]	9.33 ± 0.024	8.95[l]
1-methylpyrrolidine	25.00	0.807 ± 0.001	0.799[o]	7.95 ± 0.022	7.94[l]
piperidine (equatorial)	25.00	0.870 ± 0.001	0.857[p]	10.71 ± 0.036	9.39[l]
piperidine (axial)	25.00	0.861 ± 0.001	0.857[p]	8.66 ± 0.028	9.39[l]
1-methylpiperidine	25.00	0.821 ± 0.001	0.816[o]	8.81 ± 0.026	8.55[l]
aniline	25.00	1.036 ± 0.001	1.017[q]	12.78 ± 0.038	12.60[r]
N-methylaniline	25.00	0.975 ± 0.001	0.984[q]	12.66 ± 0.040	12.70[r]
N,N-dimethylaniline	25.00	0.937 ± 0.001	0.953[q]	11.68 ± 0.027	11.90[r]

[a] Reference 40. [b] Reference 41. [c] Reference 42. [d] Extrapolated from ref 43. [e] Reference 44. [f] Reference 45. [g] Reference 46. [h] Reference 47. [i] Reference 43. [j] Reference 48. [k] Reference 49. [l] Reference 50. [m] Reference 51. [n] Reference 52. [o] Reference 53, exptl at 20 °C, simulation at 25 °C. [p] Reference 54. [q] Reference 55. [r] Reference 56.

Figure 3. N–N radial distribution functions for liquid amines from Monte Carlo simulations with the OPLS-AA force field. X-ray results for ammonia are at +4 °C from ref 35. Successive curves are offset 3.0 units along the y-axis.

more branching is apparent for ammonia and methylamine. The numerical result for liquid ammonia is similar to the findings from prior simulations,[21,34] while hydrogen-bonding results have not been reported previously for the other amines. Furthermore, integration of the ammonia N–N rdf from the pure liquid simulations out to the first minimum at ca. 4.85 Å encompasses 11.5 neighbors. For comparison, the X-ray results of Narten at 4 °C yield 12.0 neighbors from integration of the N–N rdf to the minimum at 5.0 Å.[35]

Free Energies of Hydration. Results from the MC/FEP simulations for the relative free energies of hydration of the four prototypical amines are recorded in Table 8. The calculated values are in excellent agreement with experiment. Methylamine is the most hydrophilic and the large increments upon increasing methylation obtained previously (Table 1) have been appropriately ameliorated. Plots of ΔG vs λ are shown for the

(34) Jorgensen, W. L.; Ibrahim, M. *J. Am. Chem. Soc.* **1980**, *102*, 3309–3315.
(35) Narten, A. H. *J. Chem. Phys.* **1977**, *66*, 3117–3120.

perturbations in the gas phase, water, and chloroform for the three interconversions in Figure 4. The smoothness of the free-energy profiles, which were obtained using a $\Delta\lambda$ of 0.05 for most windows, attests to the high precision that can be obtained for such MC/FEP calculations with the BOSS program.

Rdfs and energy pair distributions for the four prototypical amines in water were analyzed to clarify the variations in hydrogen bonding and free energies of hydration. The first peaks in the N–HW rdfs (amine N–water H) are well-resolved in Figure 5 and integration to the minima at 2.5 Å yields estimates of the number of N–HW hydrogen bonds: 1.23 for ammonia, 1.20 for methylamine, 1.05 for dimethylamine, and 1.09 for trimethylamine. Thus, not surprisingly, each amine is accepting roughly one hydrogen bond from a water molecule. Hydrogen-bond donation is characterized by the H(N)–OW rdfs in Figure 6; the first peak can be assigned to hydrogen bonds with the amine hydrogens, while the larger second peak near 3.5 Å arises from the oxygen of the water that is donating a hydrogen bond to the nitrogen. The first peaks are not as sharp and well-defined as in the N–HW rdfs since amines are significantly better hydrogen-bond acceptors than donors (Table 6). Integration to the first minimum near 2.5 Å in the H(N)–OW rdfs yields estimated numbers of hydrogen bonds of 1.31 for methylamine and 0.82 for dimethylamine. For ammonia, the first peak has become a shoulder, but integration to the same limit yields an estimate of 1.38 hydrogen bonds. Combining the results for both types of interactions yields estimates of the total number of hydrogen bonds with water of 2.61 for ammonia, 2.51 for methylamine, 1.87 for dimethylamine, and 1.09 for trimethylamine. If the hydrogen bonds had similar strengths, these decreasing numbers of hydrogen bonds could lead to the erroneous order of increasing hydrophobicity with increasing methylation.

However, variations in the hydrogen-bond strengths are apparent in the energy pair distributions in Figure 7. Hydrogen bonds are reflected in the low-energy bands in such plots. Integration to the well-defined minima near −3.5 kcal/mol yields the following numbers for hydrogen bonds: 1.00 for ammonia, 1.11 for methylamine, 1.18 for dimethylamine, and 1.04 for trimethylamine. Clearly, this is the peak for the hydrogen-bond donating water molecule. Moreover, the average strength of this interaction increases with increasing methylation until it levels

Table 8. Relative Free Energies (kcal mol^{-1}) of Hydration (water), Solvation (chloroform), and Transfer (Water → Chloroform), and Δlog P for Amines at 25 °C

perturbation (A → B)	$\Delta\Delta G_{hyd}$ (water)		$\Delta\Delta G_{solv}$ (CHCl$_3$)		$\Delta\Delta G_{trans}$		Δlog P^a	
	calcd	exptl[b]	calcd	exptl[c]	calcd[d]	exptl[e]	calcd	exptl[e]
methylamine → ammonia	0.11 ± 0.20	0.26	1.10 ± 0.10	0.8	0.99 ± 0.22	0.49	0.73 ± 0.22	0.36
dimethylamine → methylamine	−0.10 ± 0.18	−0.27	0.99 ± 0.14	0.5	1.09 ± 0.23	0.79	0.80 ± 0.23	0.58
trimethylamine → dimethylamine	−1.53 ± 0.15	−1.06	0.82 ± 0.16	0.2	2.35 ± 0.22	1.27	1.73 ± 0.22	0.93

[a] Δlog P = log P_A − log P_B. [b] References 11 and 12. [c] Reference 57. [d] $\Delta\Delta G_{trans}$(calcd) = $\Delta\Delta G_{solv}$(calcd) − $\Delta\Delta G_{hyd}$(calcd). [e] From Masterfile Database, Pomona College Medchem Project & BioByte Corp., Claremont, CA, 1994.

off for dimethylamine and trimethylamine in Figure 7. The hydrogen-bond accepting waters have weaker interactions that are in the −2.0 to −3.5 kcal/mol region, and their number naturally declines with replacement of amino hydrogens by methyl groups. Thus, qualitatively two opposing effects can be inferred: increased contribution from hydrogen-bond acceptance and diminished contribution from the weaker hydrogen-bond donation with increasing methylation. With thanks to the availability of the ab initio LMP2 results (Table 6), the proper balance of hydrogen-bond strengths is achieved with the OPLS-AA force field and leads to the correct order of free energies of hydration. If, for example, the amines are too good as hydrogen-bond donors, as with AMBER*, then the latter effect dominates and hydrophobicity will increase incrementally with increasing methylation.

The concern over the disagreement between prior computation and experiment for amine hydration has also been emphasized in a recent paper by Miklavc.[36] It was argued that the errors could be explained by inadequate sampling of the torsional motion for the amines in the aqueous FEP calculations, which would lead to an R ln 3 underestimate in ΔS for each methyl rotor. That is, the FEP calculations in water would only sample one of the three equivalent rotameric states for conversion of a hydrogen into a methyl group, while all three conformational states would be sampled in a gas-phase FEP calculation. Thus, the gain in the number of states would be missed in water. This is not correct, since the three equivalent rotational states for each methyl group in amines and other organic molecules are fully sampled in any MD or MC simulations of normal length. Actually, the real problem is that FEP calculations would yield the same free energy change for conversion of a hydrogen to a methyl group in which the methyl group rotated freely or was locked in one conformational well by poor sampling or by a modified torsional potential. The ΔG contribution from a change in number of conformational states, m and n, for two systems A and B only becomes apparent through full characterization of all available conformational states of A and B and their relative free energies (eq 10), as discussed elsewhere.[37]

$$\Delta G(A \to B) = -RT \ln[\sum_{i}^{m} \exp(-G_i^B/RT)/\sum_{j}^{n} \exp(-G_j^A/RT)] \quad (10)$$

Another View: Energy Components from Linear Response. An alternative way to analyze the variations in free energies of hydration comes from linear response calculations. We have used eq 11 to estimate free energies of hydration from the results of MC simulations for a solute in water

$$\Delta G_{hyd} = \beta\langle E_{Coul}\rangle + \alpha\langle E_{LJ}\rangle + \gamma\langle SASA\rangle \quad (11)$$

where E_{Coul} and E_{LJ} are the Coulombic and Lennard-Jones energy components of the total solute−water interaction energy, SASA is the solute's solvent-accessible surface area using a probe radius of 1.4 Å for water, and β, α, and γ are empirical parameters.[38a,b] The earlier studies have been expanded with results for 44 diverse organic solutes in water including the four prototypical amines, all modeled using the OPLS-AA force field in MC simulations with 500 TIP4P water molecules.[38c] The optimized parameters are $\beta = 0.463$, $\alpha = 0.410$, and $\gamma = 0.0193$ kcal/mol Å^2. The fit yields an average unsigned error of 0.74 kcal/mol for the 44 predicted free energies of hydration in comparison to the experimental data, which cover a 13 kcal/mol range.

Notably, the predicted ΔG_{hyd} values for the amine series nicely parallel the experimental data, as summarized in Table 9. The results show that the Lennard-Jones interactions become more favorable and the surface-area term (penalty for cavity formation) becomes more unfavorable with increasing methylation. In fact, the variations of these two components are almost exactly compensating, and the pattern in total free energies of hydration parallels the changes in the Coulombic solute−water interactions. This again emphasizes the importance of the hydrogen-bond strengths. It also supports the above analysis that the trend in free energies of hydration can be attributed to the opposition of better hydrogen-bond acceptance and poorer hydrogen-bond donation with increasing methylation of the amines. The optimal point happens to occur for methylamine.

Free Energies of Transfer and Δlog P Results. As a further test of the transferability of the OPLS-AA parameters, FEP calculations were also were performed for the amine series in chloroform (Table 8). The free energy of transfer of a solute i between water and chloroform is related to its partition coefficient (P_i) via eq 12.

$$\Delta G_{trans}(i) = -2.3RT \log P_i = \Delta G_{solv}(i) - \Delta G_{hyd}(i) \quad (12)$$

Computation of relative free energies of solvation in both solvents then allows direct comparison with experimentally determined log P values by eq 13.[18]

$$\Delta\Delta G_{trans}(A \to B) = \Delta\Delta G_{solv}(A \to B) - \Delta\Delta G_{hyd}(A \to B) = 2.3RT(\log P_A - \log P_B) \quad (13)$$

In Table 8, the MC/FEP results are in good accord with the experimental relative free energies of solvation in chloroform. In this case the free energy of solvation becomes steadily more favorable, although by a diminishing amount, with increasing methylation. Combination with the computed results in water then leads to reasonable agreement between the simulation results and experiment for the relative log P values. Thus, the present MC simulations with the OPLS-AA force field repro-

(36) Miklavc, A. *J. Chem. Inf. Comput. Sci.* **1998**, *38*, 269−270.
(37) (a) Straatsma, T. P.; McCammon, J. A. *J. Chem. Phys.* **1989**, *90*, 3300−3304. (b) Jorgensen, W. L.; Morales de Tirado, P. I.; Severance, D. L. *J. Am. Chem. Soc.* **1994**, *116*, 2199−2200.

(38) (a) Carlson, H. A.; Jorgensen, W. L. *J. Phys. Chem.* **1995**, *99*, 10667−10673. (b) McDonald, N. A.; Carlson, H. A.; Jorgensen, W. L. *J. Phys. Org. Chem.* **1997**, *10*, 563−576. (c) Jorgensen, W. L., to be published.

(a)

(b)

(c)
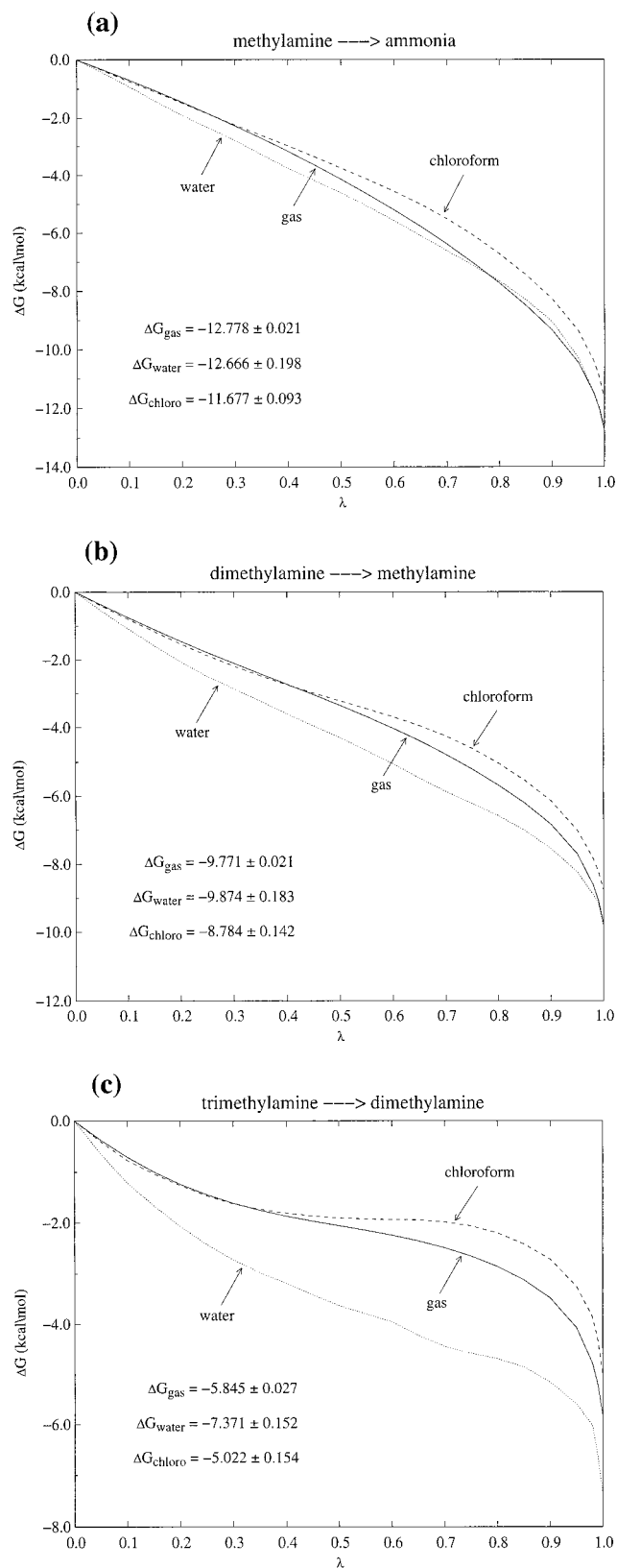
Figure 4. Plots of ΔG (kcal mol^{-1}) vs λ in the gas phase, water, and chloroform from free-energy perturbation calculations with the OPLS-AA force field: (a) methylamine $\rightarrow$ ammonia, (b) dimethylamine $\rightarrow$ methylamine, (c) trimethylamine $\rightarrow$ dimethylamine.

duce the expected order of free energies of solvation in a non-polar solvent as well as the unusual order in water.

Previously, Dunn and Nagy performed MC/FEP simulations for the conversion of methylamine to dimethylamine in water
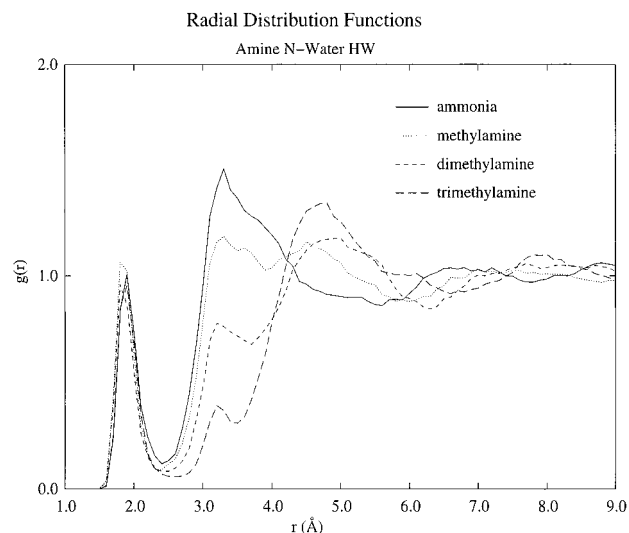

Figure 5. N$-$HW (amine N$-$water H) radial distribution functions in TIP4P water from MC simulations with the OPLS-AA force field.
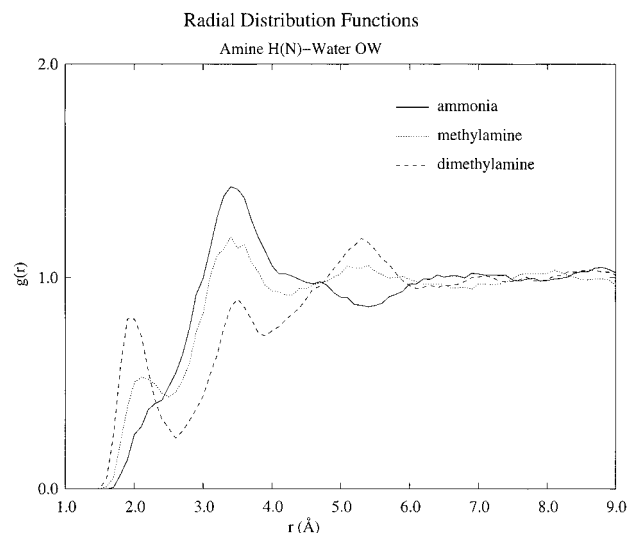
Figure 6. H(N)$-$OW (amine H$-$water O) radial distribution functions in TIP4P water from MC simulations with the OPLS-AA force field.

and chloroform.[39] A relative log P of 2.5 was obtained, which is too large in comparison with the experimental value of 0.6

(39) Dunn, W. J., III; Nagy, P. I. *J. Comput. Chem.* **1992**, *13*, 468−477.
(40) Haar, L.; Gallagher, J. S. *J. Phys. Chem. Ref. Data* **1978**, *7*, 635.
(41) Felsing, W. A.; Thomas, A. R. *Ind. Eng. Chem.* **1929**, *21*, 1269−1272.
(42) Aston, J. G.; Siller, C. W.; Messerly, G. H. *J. Am. Chem. Soc.* **1937**, *59*, 1743−1751.
(43) Swift, E., Jr. *J. Am. Chem. Soc.* **1942**, *64*, 115−116.
(44) Reid, R. C.; Prausnitz, J. M.; Sherwood, T. K. *The Properties of Gases and Liquids*, 3rd ed.; McGraw-Hill: New York, 1977.
(45) Letcher, T. M. *J. Chem. Thermodyn.* **1972**, *5*, 159−173.
(46) *CRC Handbook of Chemistry and Physics*, 72nd ed.; Lide, D. R., Ed.; CRC: Boca Raton, FL, 1991−1992.
(47) Aston, J. G.; Eidinoff, M. L.; Forster, W. S. *J. Am. Chem. Soc.* **1939**, *61*, 1539−1543.
(48) Aston, J. G.; Sagenkahn, M. L.; Szasz, G. J.; Moessen, G. W.; Zuhr, H. F. *J. Am. Chem. Soc.* **1944**, *66*, 1171−1177.
(49) Barb, W. G. *J. Chem. Soc.* **1955**, 2564−2577.
(50) Cabani, S.; Conti, G.; Lepori, L. *Trans. Faraday Soc.* **1971**, *67*, 1933−1942.
(51) Ruzicka, L.; Salomon, G.; Meyer, K. E. *Helv. Chim. Acta* **1937**, *20*, 109−128.
(52) Helm, V. R.; Lanum, W. J.; Cook, G. L.; Ball, J. S. *J. Am. Chem. Soc.* **1958**, *62*, 858−861.
(53) Lanum, W. J.; Morris, J. C. *J. Chem. Eng. Data* **1969**, *14*, 93−98.
(54) Nakanishi, K.; Wada, H.; Touhara, H. *J. Chem. Thermodyn.* **1975**, *7*, 1125−1130.

Energy Pair Distributions

Solute (amine) – Solvent (water)
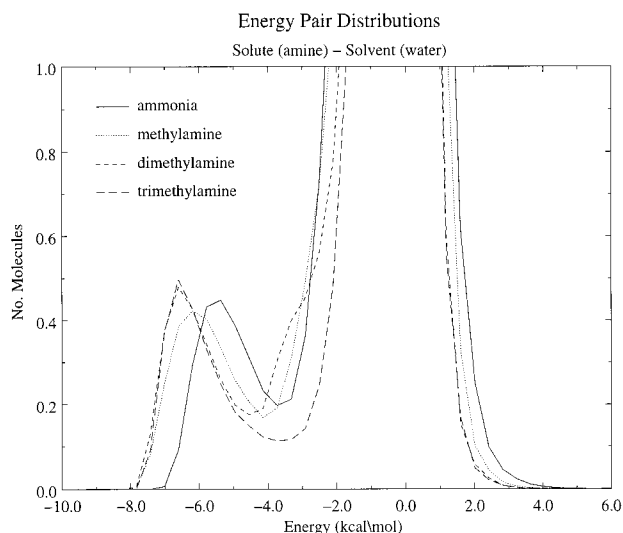
Figure 7. Solute−solvent (amine−water) energy pair distributions from MC simulations with the OPLS-AA force field. The *y*-axis records the number of water molecules per kcal mol^{-1}, which interact with the amine solute with the interaction energy given on the *x*-axis.

Table 9. Linear Response Components (kcal/mol) for Amines in Water

amine	ΔG_{Coul}	ΔG_{LJ}	ΔG_{SASA}	calcd, ΔG_{hyd}	exptl[a], ΔG_{hyd}
ammonia	−6.41	+0.41	2.66	−3.34	−4.31
methylamine	−6.87	−0.46	3.49	−3.84	−4.57
dimethylamine	−6.50	−1.26	4.23	−3.53	−4.30
trimethylamine	−5.05	−2.32	4.96	−2.41	−3.24

	$\Delta\Delta G_{Coul}$	$\Delta\Delta G_{LJ}$	$\Delta\Delta G_{SASA}$	calcd, $\Delta\Delta G_{hyd}$	exptl[a], $\Delta\Delta G_{hyd}$
ammonia	0	0	0	0	0
methylamine	−0.46	−0.87	0.83	−0.50	−0.26
dimethylamine	−0.09	−1.67	1.57	−0.19	+0.01
trimethylamine	+1.36	−2.73	2.30	+0.93	+1.07

a References 11 and 12.

or the 0.8 obtained here. The problem comes mostly from the methylamine to dimethylamine perturbation in water, which gave a ΔG of 2.90 kcal/mol vs the experimental value of 0.3 kcal/mol.[39] McDonald et al. computed free energies of solvation in chloroform for methylamine, dimethylamine, and trimethyl-

amine, by using MC/FEP simulations with OPLS Lennard-Jones parameters, but with RHF/6-31G* CHELPG charges.[38b] The computed $\Delta\Delta G_{solv}$ values in chloroform were 1.3 and 1.1 kcal/mol for the dimethylamine to methylamine and trimethylamine to dimethylamine conversions, respectively, which agree with the experimental data by ca. 0.3 kcal/mol less well than the present results (Table 8).

Conclusions

Previous computational efforts on amine hydration have employed models with standard pairwise additive interaction potentials,[9,10,14] explicit polarization,[10,15] and quantum mechanical SCRF calculations.[16,17] Although all studies with explicit solvent molecules and most SCRF models failed to mirror the experimental trends in free energies of hydration, the present work has shown that a simple, classical force field, which is parametrized to reproduce experimental properties of pure liquids (Table 7) as well as ab initio hydrogen-bond strengths (Table 6), can solve the amine hydration problem (Table 8). There is no need for models with more complex functional forms including explicit polarization. The present parametrization of the critical nonbonded terms involved few unique parameters and features simple charge increments upon increasing methylation in the amine series (Table 5). The results of the Monte Carlo simulations also led to the explanation of the observed variation in free energies of hydration through two competing trends, increased contribution from hydrogen-bond acceptance and diminished contribution from hydrogen-bond donation with increasing methylation of the amines.

In further testing, the present force field was shown to yield excellent results for properties of thirteen additional liquid amines (Table 7). The transferability of the parameters to less polar solvents such as chloroform was also demonstrated by computation of relative log *P* values in reasonable agreement with experiment (Table 8). In view of the very common occurrence of amines in chemotherapeutics, the availability of a force field with such broad, documented success for a wide range of properties in different media is most important for computer-aided drug design. Errors in partitioning between water and low-dielectric media may be expected to adversely affect predictions on protein−ligand binding as well as QSAR analyses.

JA984106U

(55) Le Fevre, J. W. *J. Chem. Soc.* **1935**, 773−779.
(56) Vriens, G. N.; Hill, A. G. *Ind. Eng. Chem.* **1952**, *44*, 2732−2735.
(57) Giesen, D. J.; Chambers, C. C.; Cramer, C. J.; Truhlar, D. G. *J. Phys. Chem. B* **1997**, *101*, 2061−2069.
(58) Davidson, W. R.; Kebarle, P. *J. Am. Chem. Soc.* **1976**, *98*, 6133−6138.